EUROPEAN ORGANIZATION FOR NUCLEAR RESEARCH

LHCb 2004-XXX, RICH
September 23, 2004

Refractive index inhomogeneity within an aerogel block

Abstract

The problem of evaluating local inhomogeneities of the refractive index inside aerogel blocks to be used as Cherenkov radiators in high energy particle physics experiments is presented. Two approaches have been investigated. The first is a purely optical method which looks for small deviations from the straight path of a laser beam entering the aerogel normal to the surface. The second method uses the Cherenkov effect itself by shooting an ultra relativistic collimated electron beam onto different points of the aerogel surface and looking for differences in the Cherenkov photons distribution.

1 Introduction

Aerogel is an appealing material for Cherenkov detectors. It is solid, made of SiO_2 [1, 2, 3] and with an extremely low density. It is transparent and its refractive index can be tuned during the production phase within the wide range of 1.008 - 1.08. Depending on the manufacturing procedure, the final product can be hygroscopic or hydrophobic.

The use of aerogel as radiator for RICH detectors [4] demands extremely good and uniform optical quality [5, 6, 7]. This has now been achieved [8], and several experiments have built RICH detectors with aerogel, like HERMES [9] or plan to build one, like LHCb [10], AMS [11] and BELLE [12].

In this note, the problem of inhomogeneities of the refractive index inside aerogel blocks is presented.

2 Refractive index uniformity

A good reason which makes silica aerogel appealing for RICH detectors is that its refractive index n can be tuned during the production phase [13]. In particular, the refractive index and the density ρ are related by the following relation:

$$n\left(\lambda\right) = 1 + k\left(\lambda\right)\rho \tag{1}$$

where k is a wavelength-dependent coefficient. Typically, if the density is expressed in g/cm^3, $k = 0.21$ at $\lambda = 632$ nm. The knowledge of this coefficient is necessary for a fast and simple refractive index control during production.

Local density inhomogeneities occurring in the production phase lead to point to point variations of the refractive index within the monoliths. These variations contribute to the Cherenkov angle θ_C uncertainty in RICH detectors. For LHCb aerogel, the maximum rms variation $\sigma(n-1)/(n-1)$ allowed is 1%, corresponding to an uncertainty $\sigma(\theta_C) \simeq 1.17$ mrad for $n = 1.030$. With this kind of spread on n, the contribution to the total resolution on the Cherenkov angle due to inhomogeneities is not the dominant one.

A method [14] to study possible refractive index inhomogeneities, shown in Fig. 1, uses a laser beam directed perpendicular to the aerogel surface in order to measure deviations from the straight optical path; the deviation angle δ is proportional to the refractive index gradients, $\mathrm{d}n/\mathrm{d}y = n \cdot \delta/t$, where t is the thickness of the block. Scanning $\delta\left(y\right)$ along a direction y, the integrated variation can be determined:

$$\Delta n\left(y\right) = \frac{n}{t} \cdot \int_{y_0}^{y} \delta\left(y\right) \mathrm{d}y. \tag{2}$$

Fig. 2 shows the result of one such measurement.

The biggest limitation of this method is that only one wavelength at a time can be monitored, and in any case a limited number of wavelengths can be used.

An alternative method which makes use of a charged particle beam to test the uniformity of the refractive index have also been developed. A setup has been installed at the

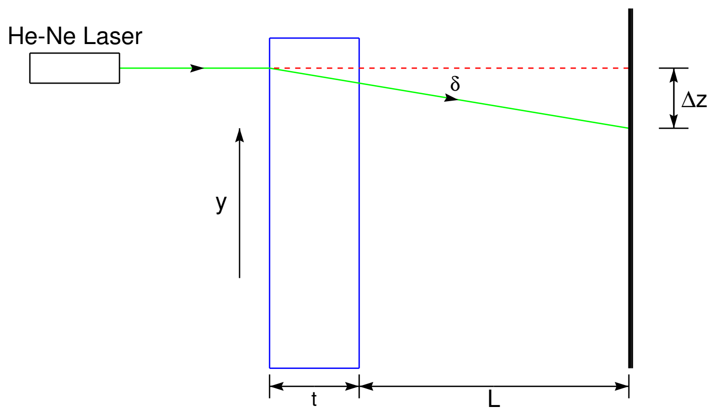

Figure 1: Setup for the laser beam method used to study the refractive index uniformity.

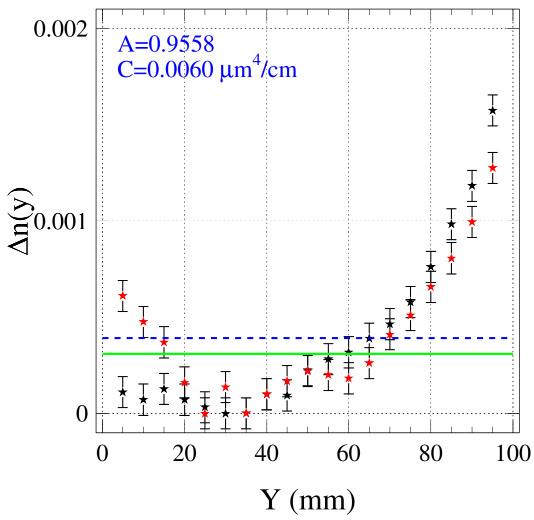

Figure 2: Result of a scan of a tile with the laser deflection method. The solid line shows the maximum $\sigma(n)$ allowed by the specifications, the dotted line shows the value of $\sigma(n)$ measured for that particular tile. The two data series refer to scans in two orthogonal directions on a $100 \times 100 \times 41$ mm^3 tile.

500 MeV electron beam of the DAΦNE Beam Test Facility in Frascati [15]. The electron beam, producing saturated Cherenkov rings in the aerogel, is used to scan the index of refraction varying the entrance point of the beam in the aerogel block. Black & white photographic films[1] have been used as photodetectors. After each run of data taking, these films have been processed by a professional photographic laboratory, scanned and processed for the data analysis. This method exploits the Cherenkov effect itself, and it is therefore appropriate to check directly the influence of refractive index variations con-

[1]Kodak® Professional TRI-X 400 Film/400TX

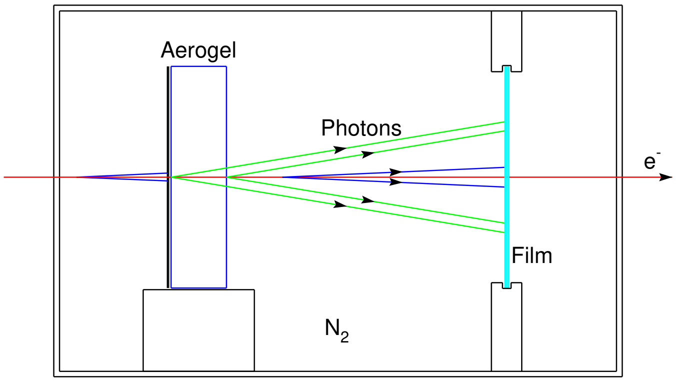

Figure 3: A schematic view of the configuration adopted for the APACHE I runs.

voluted with the emission spectrum on the Cherenkov angle reconstruction performance.

3 APACHE I

The acronym APACHE, which stands for *Aerogel Photographic Analysis by Cherenkov Emission*, has been adopted for the beam tests performed at the BTF. During the APACHE I runs, a proximity focusing configuration has been chosen to simplify the installation and data analysis, to get a quick feedback on the potential of the method.

Fig. 3 shows the layout of the setup used for APACHE I. A 25 mm thick polymethylmetacrylate (PMMA) plate is the base of the setup, whose sides are used as reference directions for alignment purposes. On top of this thick plate a dark room is mounted to prevent spurious light in the hall to interfere with the experiment. Inside the dark room, another PMMA plate is the mounting base for the aerogel support and the film holder. Everything inside the dark room is painted black to avoid reflection of scattered Cherenkov photons.

The tile is placed on a platform with the wide faces perpendicular to the beam axis. Downstream and parallel to the aerogel, the photographic film is mounted on a frame with blinds at a distance of 30 cm, such that the ring size is the maximum that the film can fully contain. The photons emitted by electrons going through the aerogel are directly collected on the film without any focusing. The dark room volume is fluxed with nitrogen to avoid as much as possible a variation of the optical properties of the aerogel due to the absorption of humidity [16].

Rayleigh scattering, whose cross sections scales as λ^{-4}, is the dominant contribution to the total diffusion probability inside aerogel. Runs have been taken with and without a UV filter to investigate possible advantages of absorbing the highest energy photons.

After developing and scanning, the film looks like the one showed in Fig. 4. Two concentric rings are clearly visible in the image. The small one contains the Cherenkov photons emitted in nitrogen between the aerogel and the film. During data analysis, the centre of gravity of the light distribution in the inner ring is taken as the intersection point of the electron beam trajectory and the film surface. The large ring contains the Cherenkov photons emitted inside the aerogel.

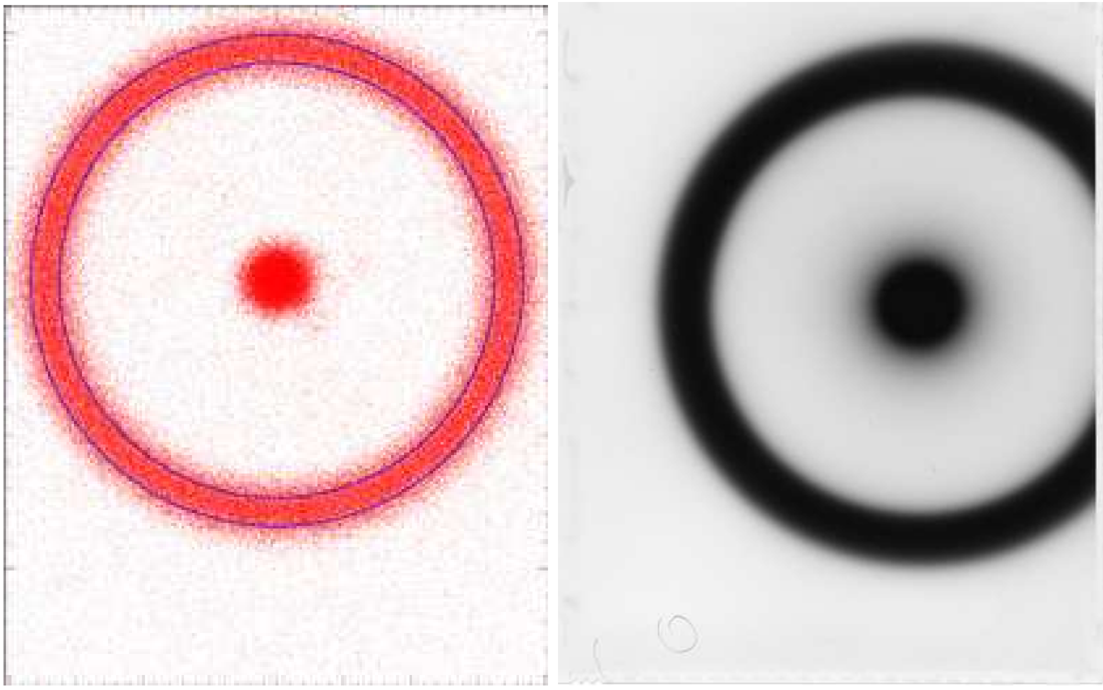

Figure 4: On the left, a GEANT4 simulation of the photon distribution on the film for an APACHE run. Superimposed to the scatter plot, two circles show the edges of the distribution in the absence of scattering inside aerogel. On the right, the scanned image of a data film. Part of the aerogel ring fell outside the acceptance due to a misalignment.

The idea underlying these tests is that by letting the beam go through the aerogel entering different points on the surface, any local change in the refractive index reflects in a change of the distribution of the photons in the large ring on the film. By scanning the image and calculating the radial distribution of light intensity for each run, one can estimate the relative variations of the refractive index from point to point inside an aerogel tile. Variations in the position of the peak of the distribution indicate variations in n.

Apart from the refractive index, many parameters influence the light distribution on the film, like the direction of the electrons, the scattering probability, the aerogel thickness, the distance between the aerogel and the ring and the detection efficiency curve of the film itself. A detailed GEANT4 [17] simulation has been developed to investigate the impact of small variations of the above parameters on the distribution curve, as well as properly link refractive index inhomogeneities with measurable shifts of the radial intensity peak. A sample plot of the simulated photon distribution on a slide is shown in Fig. 4 (left).

To avoid distortions of the intensity distribution due to the film processing, a background value has been evaluated, taken as the average light intensity in a small region close to the side of the film, blinded by the film holder, therefore not exposed to Cherenkov light. The resulting distribution, after background subtraction, is then fitted with a gaussian modulated by the detection efficiency of the film, which has been estimated, on the basis of the technical specifications of the film manufacturer and general considerations on the photographic process. A grain in the film is about 1 μm^2 in size and it turns to a black point after development only if at least three photons impinge on it. The simulated photon distribution gives the probability per electron that a single grain is hit by three

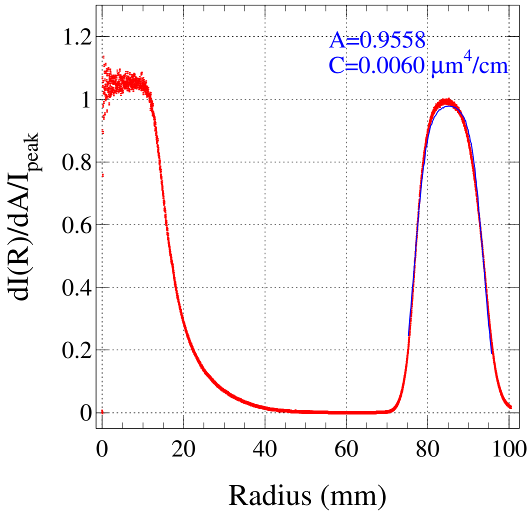

Figure 5: The plot shows the radial, peak normalised light intensity distribution on a film exposed in a typical APACHE I run, with a total fluence of about 10^{10} electrons. In blue, the distribution is fitted with a gaussian modulated by the film response function.

or more photons as a function of the radial distance of the grain from the centre of the inner ring. The quantum efficiency is taken to be flat at 100%, that is, all the photons getting to the film contribute to the above probability. The fit function has then four free parameters: the peak position and height, the gaussian spread and the integrated electron flux.

The beam intensity is measured in the BTF line by means of current measurement along the beam pipe. The measured flux and the value coming from the fit agree to within the precision (20 % ? chiedere a Mazzitelli) of the beam line measurements, which was on average 10^{10} electrons per run.

An example of one such fit is shown in Fig. 5, while Fig. 6 summarises the results of APACHE I runs on the aerogel tile.

From the simulation program, it was found that in order to detect point to point refractive index variation of the order of $\sigma(n-1) \simeq 1\%$ one needs to identify the peak position in the radial distribution plot to better than 0.25 mm, see Fig. 7.

The most limiting parameter was the thickness of the aerogel, which accounts for the largest contribution to the size of the ring, and in addition to that it is difficult to measure from point to point and it is rather sensitive to small misalignments. An upgrade was needed.

4 APACHE II

In order to improve the precision in the mean Cherenkov angle measurement and therefore have a higher resolving power in terms of refractive index inhomogeneities, a measurement campaign in a RICH configuration was performed. A light tight anodised aluminium vessel

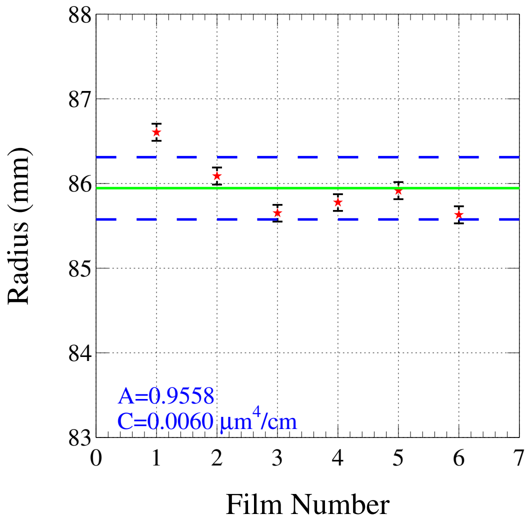

Figure 6: Summary scatter plot of the APACHE I runs taken on the same aerogel tile. The solid line is the mean value of the peak position for each film. The dotted lines give the one-sigma region around the mean value.

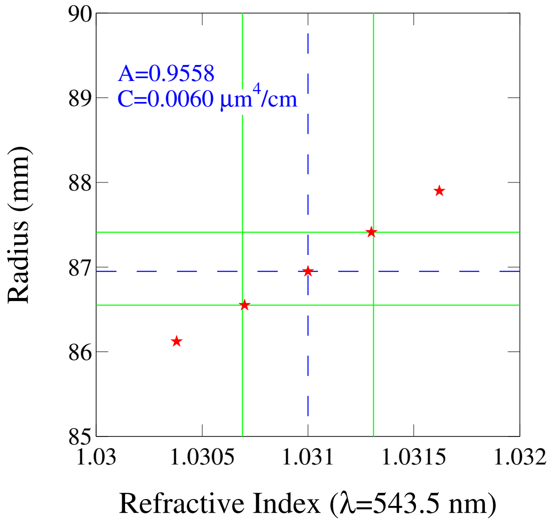

Figure 7: Displacement of the radial peak position for refractive index variations in steps of 1%. The dotted lines correspond to the nominal n and R, the solid lines are the $\pm 1\%$ region.

replaced the dark room, and a tilted spherical mirror in front of the aerogel was introduced to focus the Cherenkov photons on the film, placed outside the beam in the focus of the mirror. A sketch of the setup is shown in Fig. 8.

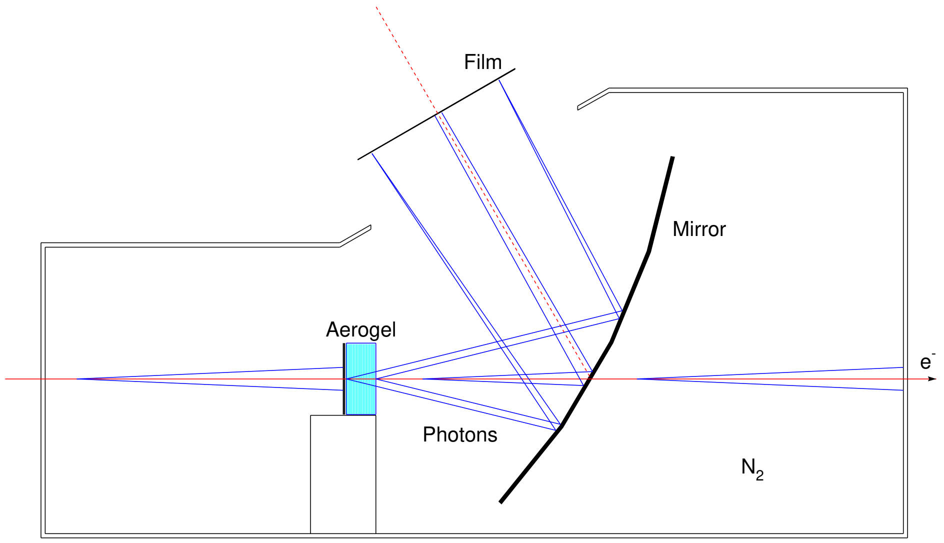

Figure 8: A schematic view of the setup built for the APACHE II runs.

It is no longer possible to make a sensible radial distribution of the light intensity, but one can track back the photons [18] from the impinging point on the film and plot directly the Cherenkov angle distribution. The spherical mirror ideally focuses all the photons with parallel trajectory to one point in the focal surface, independent of the emission point and consequently of the aerogel thickness. This is not quite the case for a real mirror, where spherical aberrations distort the focusing properties in a non trivial way. In addition to that, the tilt of the mirror axis with respect to the electron beam direction introduces a small uncertainty in the angle measurement due to the emission point position inside the aerogel. However, even with those limitations, the RICH configuration provides a far superior performance to the proximity focus one. Moreover, in view of a future use of Hybrid Photo Diodes (HPD) as photon detector, it is wise to have a setup that allows to place them outside the electron beam.

A new GEANT4 simulation has been developed according to the APACHE II setup Fig. 9 is an example of a simulated run (left) and a scanned image of the film used in an actual APACHE II run (right). With respect to the results obtained in APACHE I the two rings are neater, but distorted by the spherical aberrations.

The hit-by-hit retracking algorithm allows to build the distribution of the reconstructed Cherenkov emission angle. Such distribution is plotted in Fig. 11. These plots give the average shift of the mean reconstructed Cherenkov angle from film to film, and therefore from point to point. The parameter chosen for comparison among runs is the angle for which the distribution has a maximum in the aerogel ring region. The analysis of simulated data shows, Fig. 10, gives the link between a refractive index change and the corresponding shift in the reconstructed Cherenkov angle peak.

To study the uncertainties associated with this method the simulation program was run in order to estimate the effect of small changes in the setup geometry or beam conditions. The beam direction has been varied both as parallel displacement and as a tilt with respect to the nominal beam axis. The film position in space has been varied in order to check the effect of systematic shifts in the reconstruction parameters in the analysis.

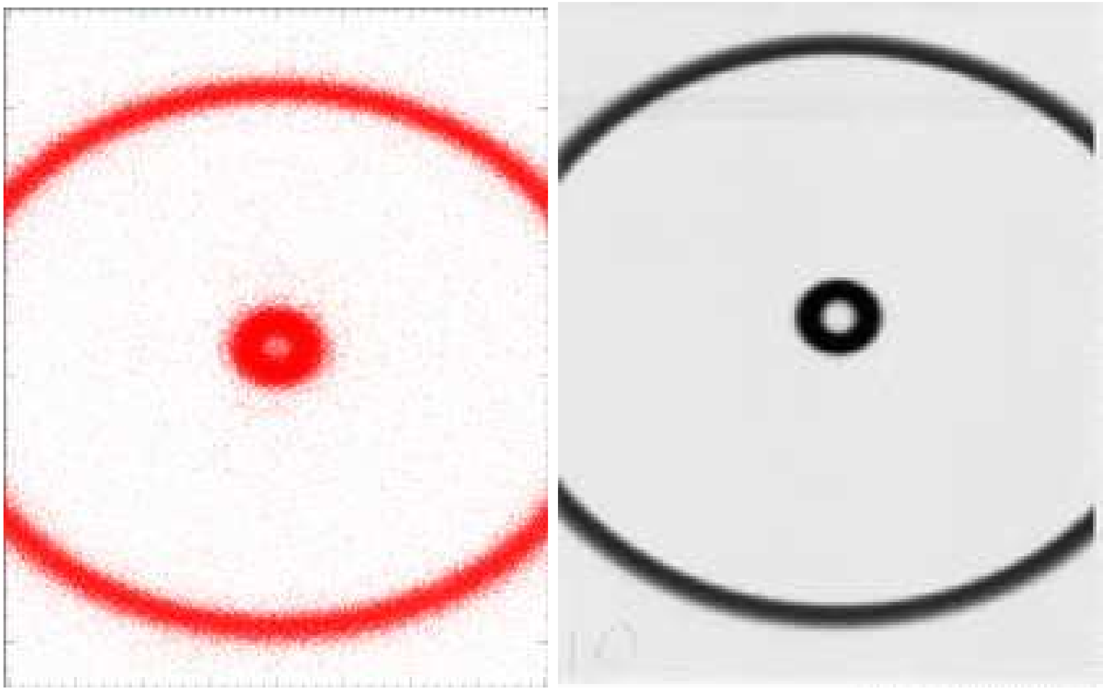

Figure 9: On the left, GEANT4 simulation of the photon distribution on the film for an APACHE II run. On the right, the scanned image of a data film. The two sides of the aerogel ring fell outside the acceptance.

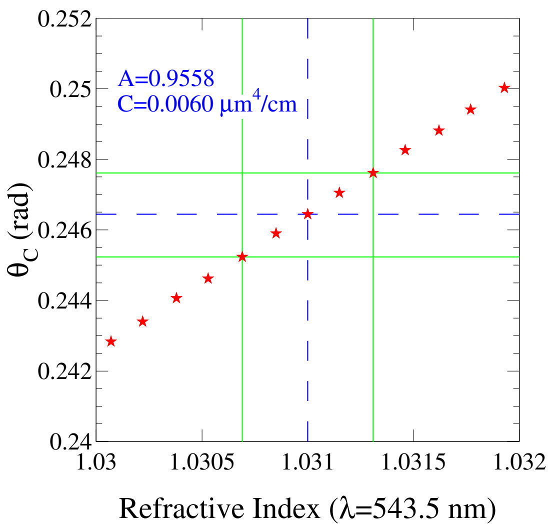

Figure 10: Displacement of the reconstructed Cherenkov angle peak position for refractive index variations in steps of 0.5%. The dotted lines correspond to the nominal n and Θ_{C}, the solid lines are the $\pm 1\%$ region.

Since the aim of the experiment is a scan of relative variations of n, it has been found out that small misalignments do not contribute substantially to our accuracy, as long as the conditions are stable from run to run. To check the stability of the conditions, a good indicator is the Cherenkov angle distribution for photons produced in the nitrogen volume between the aerogel and the mirror. Incidentally, it is relevant to point out that a black carton screen was placed just upstream the aerogel to prevent the photons emitted in nitrogen to go through the tile and be scattered. The value of the angle for which the nitrogen ring has a maximum, then, is independent of the aerogel, and it is expected to be constant from run to run, apart for tiny refractive index variations due to temperature and pressure changes. Any significant displacement of the nitrogen Cherenkov peak is then to be ascribed to uncontrolled variations of the run conditions. It has been verified in a thorough simulation campaign that the resolution in the peak position is 0.3 mrad. The contributions to the resolution are listed in table 1.

Source	Contribution to the resolution (mrad)
Beam divergence	0.1
Beam shift	0.1
Beam tilt	0.2
Film position	0.2
Total	0.3

Table 1: List of contributions to the angular peak resolution in APACHE II.

The scan performed on the sample aerogel block consisted in chosing 15 points on the surface as entrance points of the beam: the tile falls inside the specifications, with a measured $\sigma(\theta) = 1.14$ mrad, where $\sigma(\theta)$ stands for the variance of the angular peak positions in all the films, as shown is Fig. 12.

References

[1] M. Cantin et al., Nucl. Instr. and Meth., **A118** (1974), 177.

[2] A. F. Danilyuk et al., Nucl. Instr. and Meth., **A433** (1999), 406.

[3] H. Yokogawa and M.Yokoyama, J. Non-Cryst. Solids **186** (1995) 23.

[4] R. De Leo et al., Nucl. Instr. and Meth., **A401** (1997), 187.

[5] A. K. Gougas et al., Nucl. Instr. and Meth., **A421** (1999), 249.

[6] A. R. Buzykaev et al., Nucl. Instr. and Meth., **A433** (1999), 396.

[7] R. De Leo et al., Nucl. Instr. and Meth., **A457** (2001), 52.

[8] M. Y. Barnykov et al., Nucl. Instr. and Meth., **A419** (1998), 584.

[9] HERMES Coll., Nucl. Instr. and Meth., **A417** (1998), 230.

[10] LHCb Coll., LHCb RICH TDR, CERN/LHCC/2000-0037.

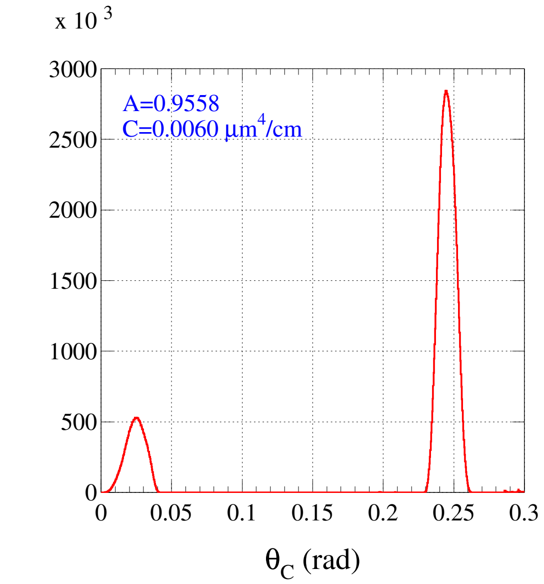

Figure 11: The Cherenkov angle distribution for an APACHE II run. The two peaks refer to photons emitted in nitrogen (low angles) and in aerogel (large angles).

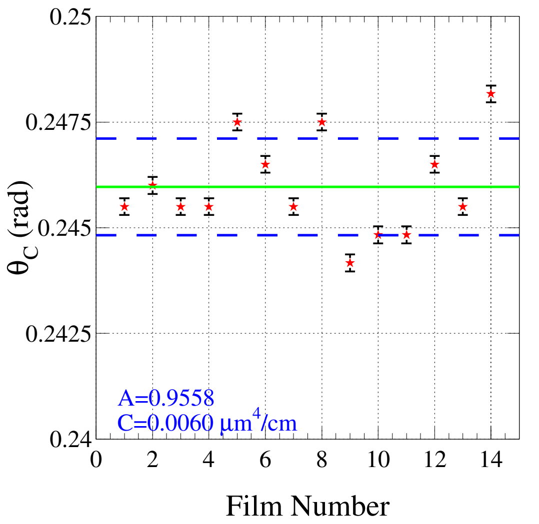

Figure 12: Summary plot of the results of all APACHE II runs on one aerogel tile. The green solid line is the mean value of the average Cherenkov angle for each film. The blue dotted lines give the one-sigma region around the mean value. With $\sigma(\theta) = 1.14$ mrad this tile falls inside the specification $\sigma(\theta) \leq 1.17$ mrad.

[11] R. Battiston *et al.*, Nucl. Instr. and Meth., **A409** (1998), 458.

[12] T. Matsumoto et al., physics/0309032 Sep. 2003

[13] A. R. Buzykaev *et al.*, Nucl. Instr. and Meth. **A379** (1996) 465.

[14] A. R. Buzykaev *et al.*, Nucl. Instr. and Meth. **A433** (1999) 396.

[15] G. Mazzitelli *et al.*, Nucl. Instr. and Meth. **A515** (2003) 524.

[16] T. Bellunato *et al.*, Nucl. Instr. and Meth. **A527** (2004) 319.

[17] S. Agostinelli *et al.*, Nucl. Instr. and Meth. **A506** (2003) 250.

[18] R. Forty *et al.*, Nucl. Instr. and Meth. **A384** (1996) 167.